Reference: *Biol. Bull.* **196:** 1–17. (February, 1999)

Dynamics of Gastrovascular Circulation in the Hydrozoan *Podocoryne carnea:* the One-Polyp Case

STEVE DUDGEON[1,*], ANDREAS WAGNER[2], J. RIMAS VAIŠNYS[3,4], AND LEO W. BUSS[3,5]

[1]*Department of Biology, California State University, Northridge, California 91330-8303;* [2]*Department of Biology, The University of New Mexico, 167A Castetter Hall, Albuquerque, New Mexico 87131-1091;* [3]*Departments of Ecology and Evolutionary Biology,* [4]*Electrical Engineering,* [5]*Geology & Geophysics, Yale University, New Haven, Connecticut 06520*

Abstract. Time-lapse video microscopy and image analysis algorithms were used to generate high-resolution time series of the length and volume of a single hydrozoan polyp before and after feeding. A polyp of *Podocoryne carnea* prior to feeding is effectively static in length and volume. At 20°C, feeding elicits 8-millihertz (mHz) oscillations in polyp length and volume. A polyp connected to a colony by a single stolon displayed an abrupt transition from low-amplitude, 8-mHz oscillations to large-amplitude, 6-mHz oscillations at 1.5–2 h after feeding. The transition was preceded by a substantial decrease in polyp volume and increase in length which coincided with the export of food items from the digestive cavity of the polyp into the colonial gastrovascular system. In contrast, 8-mHz oscillations of a polyp isolated from a colony continued for 12.7 h after feeding, at which time particulates from the digestive cavity were exported into the hydrorhiza and a 4-mHz subharmonic became briefly dominant. Regular oscillatory behavior was terminated by regurgitation at comparable intervals post-feeding in coupled and isolated polyps. These observations are compatible with the hypothesis that the presence of nutrients in the digestive cavity induces polyp oscillations and that release of nutrients into the gastrovascular system similarly induces unfed polyps to oscillate, thereby distributing the contents of the fed polyp throughout the colony.

Introduction

The gastrovascular system is the only physiological system of hydrozoans whose behavior is known to be manifested colonywide. The system transports fluid between the digestive cavities of polyps through the lumens of the endodermal canals between polyps, resulting in the colony-wide exchange of nutrients and dissolved gases. Recent studies have shown that perturbation of gastrovascular transport has marked effects upon colony ontogeny and life history. Specifically, the production of polyps and the frequency of stolon branching and anastomosis are accelerated, and the age at which medusae are produced is altered, in *Podocoryne carnea* (Sars, 1846), by perturbations of energetic metabolism that reduce the volumetric flow rate through stolons (Blackstone and Buss, 1992, 1993; Blackstone, 1997, 1998). Moreover, surgically manipulating the relative sizes of stolons within a colony of *Hydractinia symbiolongicarpus* (Buss and Yund, 1989) is sufficient to stably convert a runner-like colony into a sheet-like colony and *vice versa* (Dudgeon and Buss, 1996).

Control of vascular morphology by response to internal hydromechanical signals is increasingly well-known in vertebrate systems (Bevan *et al.*, 1995). Murray (1926) proposed that tree-like vascular designs minimize the total energy expended in propelling the fluid and maintaining the tissues. The predicted optimum is one in which the wall shear stress is constant throughout (Zamir, 1977; Sherman, 1981; LaBarbera, 1990). Several genes are known to be differentially expressed upon perturbation of wall shear stress in a fashion that adjusts vessel radii to values that restore a systemwide constant shear stress (Bevan *et al.*, 1995). Similar design optimizations and flow-dependent gene expression may underlie the response of hydrozoan colonies to altered patterns of gastrovascular transport. However, the task of identifying the relevant hydromechanical features and the patterning elements that respond to

Received 20 February 1998; accepted 25 November 1998.

* E-mail: steve.dudgeon@csun.edu

such features requires an understanding of how fluid circulates within a colony.

Unlike the vertebrates, which have a vascular system with a single pump that propels a unidirectional flow of fluid within a dichotomously branching tree, a hydrozoan colony can be composed of thousands of individual polyps connected to one another by a complex array of anastomosing stolons within which fluid may flow alternately in any direction. Understanding how an array of pumps and vessels generate a time- and space-varying distribution of metabolites and hydrodynamic signals is a considerable challenge. Our approach has been to characterize the dynamics of a single polyp, in the hope that the behavior of an isolated unit will prove simple enough to allow us to develop a mathematical model. Polyp models, when coupled by suitably developed models of the stolon, may eventually permit systematic analysis of the consequences of the arrangement of polyps in various geometries. To this end, we have documented the feeding behavior of single polyps of the colonial hydroid *Podocoryne carnea.* We present time series of the length and volume of a single isolated polyp and contrast this behavior with that of a single polyp coupled to a colony, both before and after feeding.

Materials and Methods

Animals and their maintenance

The hydrozoan *Podocoryne carnea* produces encrusting colonies of a typical filiform form. Our observations are restricted to young colonies bearing only gastrozooids (hereafter called polyps). Polyps extend upright atop the stolons, which adhere to the substratum. The polyp is the sole component of the system that can exchange fluid with both the external medium (*via* the mouth) and the rest of the gastrovascular system (*via* a contractible opening between its gastric cavity and the stolon or stolons coextensive with it). Exclusive of epithelial conductance, the gastrovascular system is the only known colonywide conducting system in this species (*i.e.,* neither a nerve net nor muscle fibers occur in the stolons; Stokes, 1974; Schierwater *et al.,* 1992).

All colonies of *P. carnea* were asexually propagated from a single clone (P34) collected at the Peabody Museum Field Station, Guilford, Connecticut, in September 1989. Colonies were grown on the surface of either glass slides (25 × 20 × 1 mm) or coverslips (484 mm^2) in 40-l aquaria containing artificial seawater (REEF CRYSTALS, Aquarium Systems, Mentor, Ohio) at 18 ± 1°C. Animals were fed to repletion twice per week on a diet of 3- to 5-day-old brine shrimp (*Artemia salina* (Linnaeus, 1758)) nauplii. Colonies were propagated asexually by surgically explanting single polyps onto the surface of a glass slide or coverslip. Explanted polyps were held in place by a loop of thread until the growth of stolons attached them to the surface.

Observational protocol

Colonies were not fed for 2 days prior to treatment and subsequent observation. Polyps growing on the edge of a glass slide were standardized to lengths of ± 100 μm, and stolons were severed as necessary to establish two treatments. For observation of isolated polyps, all stolons connecting the chosen polyp to the colony were severed so as to retain a segment of stolon roughly 800 μm long with two blind ends and the polyp positioned near the center. Severed stolons heal and become occluded instantly (Berrill, 1953). For observations of coupled polyps, all but one stolonal connection to the colony was severed. In this case, the polyp was situated about 300–400 μm from the blind end of the stolon. The size of the colony varied between replicates, but was in all cases vastly larger than the internal volume of the chosen polyp.

Following surgery, the colony was maintained under standard conditions for 12 h prior to the start of observations. The colony to be observed was then placed within a temperature-controlled chamber in 10 ml of 0.45-μm filtered seawater at 20 ± 0.1°C and viewed at 100× using a Zeiss Axiovert 35 inverted microscope. The polyp was positioned so as to provide a longitudinal profile extending from the mouth to the base of the polyp. Illumination was arranged to optically filter the tentacles, leaving only the body column visible (*i.e.,* the field was flooded with light sufficient to render the polyp outline black and the remainder of the field uniformly white). Polyp behavior was videotaped, typically for 1.5–2 h prior to feeding, using a Dage MTI camera connected to the microscope and a videocassette recorder. The polyp was then removed from the chamber, hand-fed a single newly hatched brine shrimp nauplius, returned to the chamber immediately after ingesting the food item, and videotaped for the following 24 h.

Image analysis

Images were recovered from the videotaped record of polyp behavior using a PCVISION frame grabber and OPTIMAS image analysis software. A series of programs, written in the OPTIMAS macro language, were used to extract polyp length and diameter at multiple points along the longitudinal axes from each binary image of a polyp's outline. Figure 1 and its legend illustrate the steps by which length and width measurements are generated from an image. Polyp volume was estimated from these measurements of polyp length and diameters, using the extended Simpson's rule (Press *et al.,* 1992). The macros used and an extensive discussion of the reasoning which led to their development are available at http://www.csun.edu/~sd51881.

There are three sources of error in the procedures we employ: (1) errors associated with sampling the coordinates that compose the outline of the polyp, (2) errors associated with the assumption that the polyp is rotationally symmetric

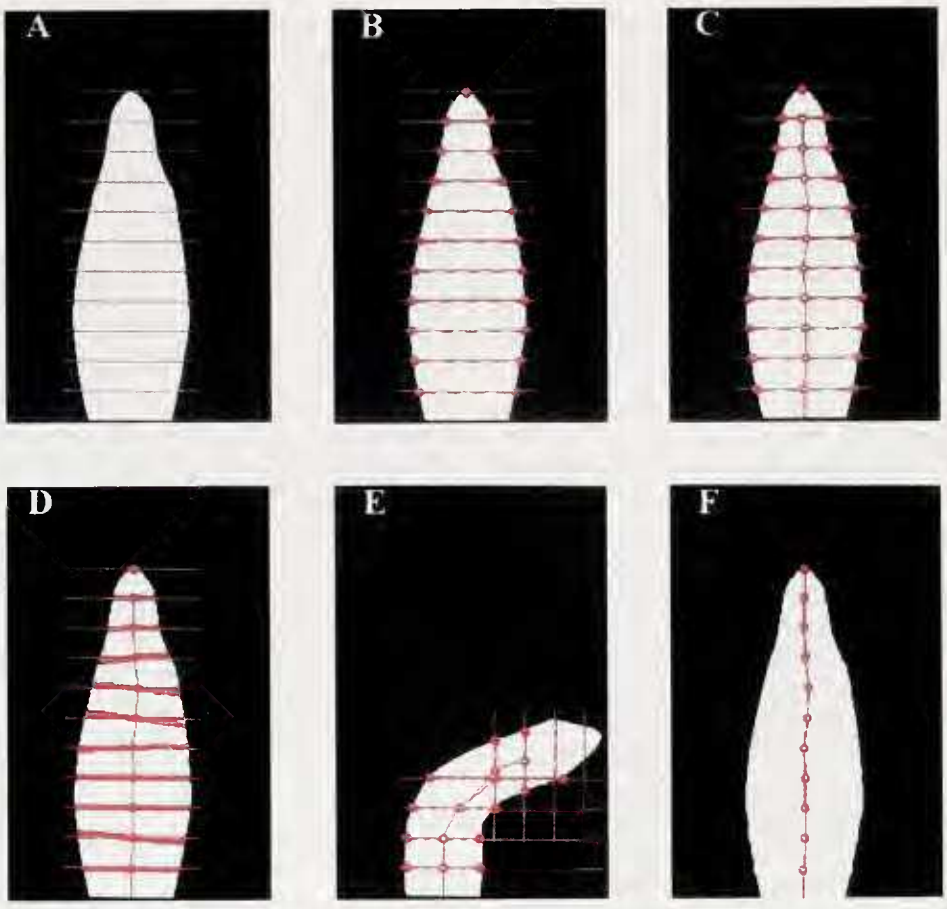

Figure 1. Steps used by image-processing algorithm following inversion of the binary image (black pixels to white and *vice versa*). (A) Establishing 11 evenly spaced transects along the longitudinal polyp axis; (B) detecting and marking the edge of the polyp at both ends of each transect line; (C) determining the midpoint of each transect line along the body column with respect to the marked edges of the polyp and connecting the midpoint segments along the longitudinal polyp axis; and (D) establishing the line normal to the midpoint-to-midpoint line segment at each transect—the length of these normal lines constitute the diameter measurements. (E) Example illustrating the switch between horizontal and vertical scans by the algorithm when a bend of the polyp exceeding 53° is detected. (F) Fitting a 4th order polynomial function to the set of midpoint coordinates for determining polyp length.

about the axis of the focal plane, and (3) errors associated with bending of the polyp outside the focal plane. The first two sources of error were estimated from an analysis of sampling efficiency and by extensive experimentation on volume fluxes observed in colonies of known stolonal volume; they constitute an error of $< 5\%$, which corresponds to an error in estimates of volume amplitude of $\pm$ 0.7 nl. The relevant experiments and data upon which this error estimate is based are available at http://www.csun.edu/~sd51881. With respect to the remaining source of error, our algorithms cannot detect the bending of polyps outside the focal plane. Such bends, however, constituted only a small fraction of the overall record (5.9% and 2.6% in the coupled and isolated records, respectively). These data points are spurious and are denoted as such by tickmarks along the abcissa in plots of the time series we present below.

Time-series analysis

Using the algorithms described above, one of the four replicates in each treatment was analyzed to generate a high-resolution time series of polyp length and estimated volume. Measurements were made at 8-s intervals from the onset of feeding to 436:09 and 1474:12 min:s post-feeding for coupled and isolated treatments, respectively.

Time-series data were analyzed using Mathematica (Version 2.2, Wolfram Research, Inc.) on a Hewlett-Packard Apollo 9000 workstation. From each raw time series of length and volume, we calculated a low- and high-pass-filtered version (Priestley, 1981). A low-pass-filtered time series is one from which short-term fluctuations have been removed. The low-pass-filtered time series was computed as a sliding running average, using a uniform window

spanning 201 points and centered about the point in question. The (complementary) high-pass-filtered time series was obtained by subtracting the low-pass-filtered series from the original series, giving a series with a mean of zero from which long-term drifts had been removed.

To detect trends within the time series, the high-pass-filtered series was further analyzed by examining a succession of windowed Fourier transformations. The entire high-pass-filtered time series was divided into segments ("windows") comprising 20 min of observational data, with two consecutive windows overlapped by 15 min. Fourier coefficients were estimated for each of the windows separately using a Fast Fourier transformation, and the power spectrum was calculated.

Efficient techniques for analyzing time-series data depend on having a complete time series that has been sampled at equal time intervals. If data points are missing, an error proportional to the number of missing points is introduced into the estimation of the series spectrum. In the series analyzed here, missing observations are rare; they contribute 1.90% and 0.39% to the variability in the spectrum in the coupled and isolated treatments, respectively.

"Aliasing," a frequent problem in the spectral analysis of discretely sampled time series (Priestley, 1981), does not appear to bias the spectra we present below. This conclusion was reached on the basis of an exploratory analysis in which data sampled at a higher temporal resolution did not display any qualitative changes in the spectral composition. The observation that none of the spectra derived at the chosen sampling density have any peaks in the high-frequency range support this conclusion.

Repeatability

In addition to the high-resolution time series, data were collected from the remaining three replicate video records for each treatment at the same 8-s resolution for 20-min intervals to determine whether patterns observed in the high-resolution analysis were repeatable. These 20-min intervals were chosen haphazardly, with the added criterion that the images of the polyp were of good quality with respect to contrast, brightness, and definition of the outline against the background. In both treatments, power spectra and amplitudes of length and volume oscillations were calculated for at least 1 (and up to 5) 20-min intervals in both the pre- and post-export phases of digestion for each replicate polyp.

From each power spectrum, we identified the frequency of each peak and calculated its signal-to-noise ratio as the ratio of peak height to the maximum height of noise in the plot (*i.e.,* the highest point remaining on the landscape after excluding the set of peaks). We report the frequency and the signal-to-noise ratio for only those frequencies > 3.3 and ≤ 10 mHz (millihertz). The lower frequency limit is set by the duration of the record, and the higher limit is set to avoid reporting bends and contractions as frequency signals. The upper limit of a 10-mHz frequency also excludes harmonics (if present) at twice and three times the principal frequency.

To estimate amplitude, length or volume measurements from the same 20-min window were subdivided into four segments of 5 min each (*i.e.,* approximately 2 oscillation cycles). Each of these shorter segments was viewed as an unordered sample of length or volume measurements. The difference between length (volume) at the 97.5 percent quantile and length (volume) at the 2.5 percent quantile in a segment was used as an estimate of amplitude. The mean amplitude of the four 5-min segments was used as the amplitude of length (volume) for the 20-min interval. This measure not only reflects short-term polyp oscillations, it also effectively excludes trends in length (volume) within the window and the effect of short polyp contractions.

Shape variation

We do not present extended time series of the width of each polyp cross-section. Rather, to characterize changes in polyp shape, 25 widths along the body column of the polyp were measured every 8 s for two 15-min intervals for each treatment. The first interval was taken at 90 min post-feeding in both treatments and the second at about 180 and 700 min post-feeding in the coupled and isolated treatments, respectively. The coefficient of variation of each of the widths was calculated and plotted against the position of that width along the longitudinal polyp axis.

Stolon observations

A series of observations were made on stolon behavior in an attempt to correlate features of the polyp time series with events observed within the stolons. The rationale for doing so is that the mouth of the polyp remains closed over the time periods analyzed here, hence any changes in polyp volume (exclusive of experimental error) must represent exchange with the stolon. Three replicate records were made of both isolated and coupled treatments, established as described above, but with the focal plane established adjacent to the polyp-stolon junction at 400×. We do not present detailed time series for stolonal oscillations here (see Buss and Vaišnys, 1993); rather, we use these videotapes to describe events observed in stolons at times corresponding to principal features in the polyp record.

These descriptions are supplemented with limited measurements. From the videotapes, we measured the onset of oscillations in stolon diameter after feeding and the time at which the polyp initiated export of particulates from its digestive cavity into the stolon. In addition, from frame-grabbed images we measured lumen diameters, amplitudes and frequency of stolon oscillations for three consecutive cycles preceding and following export. Measures were ob-

tained before and after feeding, but prior to export, at 30 min post-feeding in the stolons of coupled polyps and at 30 and 150 min post-feeding in the stolons of isolated polyps. Post-export measures were obtained at 150 min post-feeding in the coupled treatment and at 1 h after export in the isolated treatment. To facilitate comparisons between stolons with different diameters (Blackstone and Buss, 1992), stolon measurements were standardized to measures of the periderm-to-periderm width.

Results

Pre-feeding behavior and return to pre-feeding conditions

Prior to feeding, polyps behaved similarly in both isolated and coupled treatments. A representative record appears in Figure 2A, showing that polyp length and volume remained constant prior to feeding, exclusive of occasional volume-conserving contractions in length (*e.g.*, at $t = -22$ min). Feeding was terminated by regurgitation of undigested materials, which occurred at 18–22.5 h post-feeding in both treatments. After regurgitation, the polyp regained near-original values of length and volume (Fig. 2B; see also min 1350 in Fig. 6B). Contraction pulses and asymmetric polyp bends occurred frequently before and after regurgitation.

Polyps connected to a colony

The raw time series for both polyp length and volume is shown in Figure 3. The presentation of the time series is simplified by treatment of three different intervals:

0–15 minutes post-feeding. After ingesting the brine shrimp, the polyp contracted from about 950 to 400 μm in length, and its volume increased from about 7 to 18 nl (*cf.* Figs. 2A and 3). In the first 15 min following feeding, the polyp displayed a trend of increasing length and decreasing volume, but otherwise lacked regular behavior. At 8 min post-feeding, volume decreased sharply, from about 18 to 14 nl, coinciding with the repositioning of the brine shrimp nauplius within the digestive cavity. Coincident with the rapid decrease in volume was an apparent stabilization of volume (at *ca.* 12–14 nl) and length (at *ca.* 550 μm). Regular oscillations in both polyp length and volume began shortly after this repositioning.

15–125 minutes post feeding. The oscillatory behavior, as well as the plateau in length and volume established by 15 min post-feeding, was retained until about 100 min post-feeding. Throughout this period of oscillation, changes in polyp shape were largely restricted to variation in the width of the hypostomal region of the polyp (Fig. 4A). At 100 min, regular oscillations were interrupted as volume underwent another substantial decrease, dropping from about 14 nl to a minimum of about 5 nl at 110–120 min, only to increase to 8 nl at 125 min.

Prior to the volume decrease at 100 min, the polyp was opaque. In the interval between 95 and 105 min, the polyp became increasingly transparent, indicating an export of contents of the digestive cavity. Since no material was seen leaving the mouth, the exchange must have occurred between the polyp and the colony gastrovascular system.

125–436 minutes post-feeding. The rapid decline in volume immediately preceding this interval was followed by a change in length dynamics and a return to regular oscillatory dynamics in volume. Length, which had reached a plateau at 550 μm, began to increase to a new plateau at 750 μm. The volume oscillations commencing at 125 min were of substantially greater amplitude than those which preceded it, with changes in volume often exceeding 100% with each cycle. These pronounced oscillations were accompanied by a change in the regions of the polyp showing the greatest variation in width. In contrast to the preceding interval, during which most shape change was restricted to the hypostome, the large-amplitude oscillations characterizing this time interval displayed the largest coefficient of variation in the mid-gastric region of the body column (Fig. 4B).

Large-amplitude volume oscillations continued until about 225 min, after which they gradually declined in amplitude from up to 8 nl at the beginning of the interval to less than 2 nl at the end of the record. Polyp length over the interval spanning 170–200 min showed a gradual lengthening trend from 750 to 900 μm, after which the plateau at 900 μm in length persisted for several hours. Both contraction pulses and polyp bending became increasingly common as the amplitude of volume contractions attenuated.

Oscillations in both length and volume of the polyp throughout the feeding cycle were characterized by a single dominant frequency component (Fig. 5). The dominant component, however, shifted from an initial dominant frequency of about 8 mHz (corresponding to 1 cycle every 2 min) to 6 mHz at 125 min. This shift to the lower frequency between 125 and about 200 min coincided with the large-volume oscillations of the polyp (*cf.* Fig. 3). Weak harmonics of two and three times the dominant frequency were also present in the length spectrum during the first 100 min. Subharmonics were not evident. Because most of the volume spectrum was dominated by the massive oscillations between 125 and 200 min, oscillations before and after this period, although present, left only faint traces in the spectrum of Figure 5. No appreciable contributions to either length or volume oscillations came from frequencies greater than 24 mHz.

The frequency and amplitude of oscillations over the course of a feeding cycle were repeatable with respect to both length and volume among replicates of the coupled polyp treatment (Table 1). For all replicates, a single frequency predominated both before and after the export of the contents of the gastric cavity. Moreover, the predominant

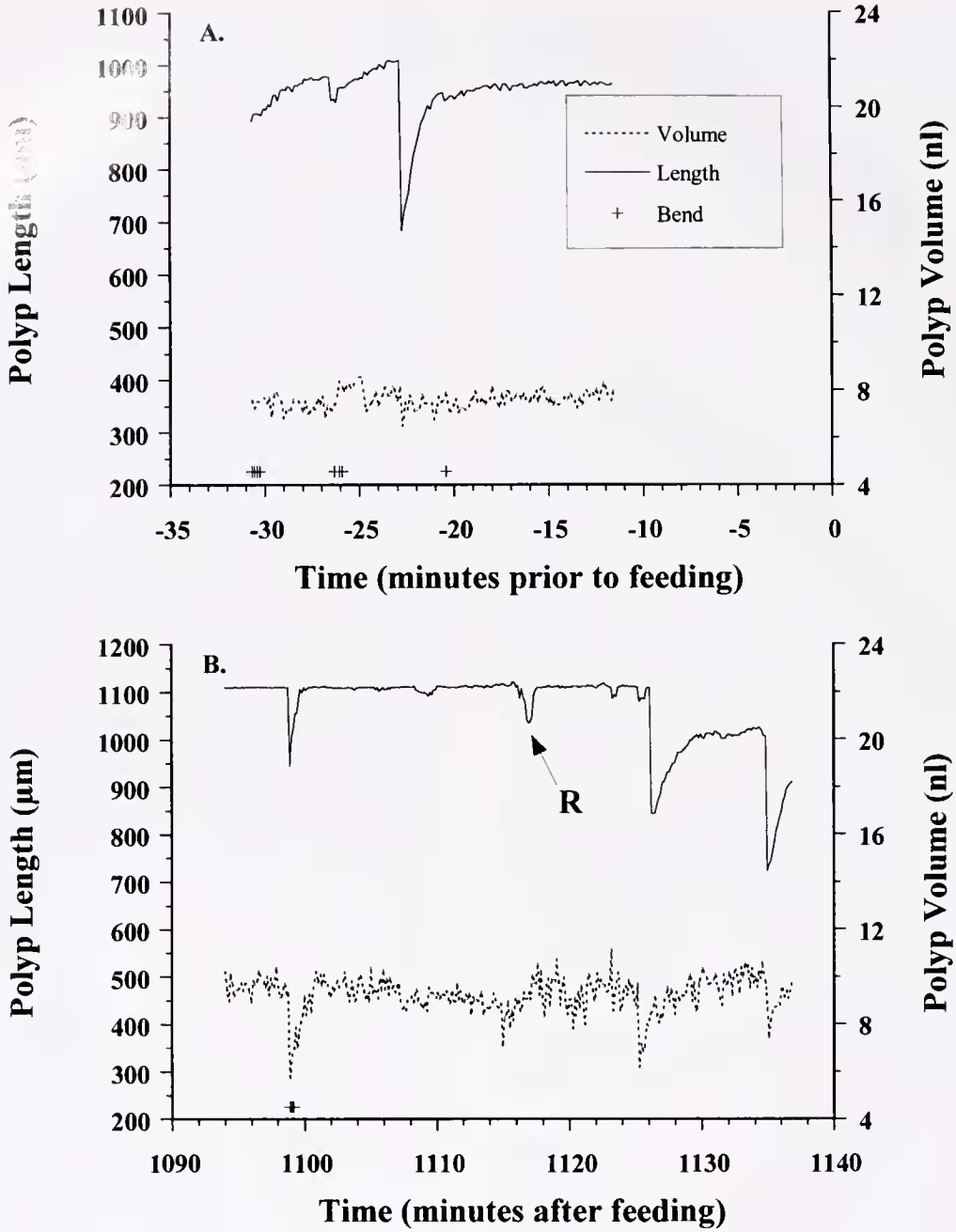

Figure 2. Time series of length (solid line) and volume (dashed line) dynamics of a polyp coupled to a colony by one stolon (A) prior to feeding and (B) at the end of digestion showing the return to initial conditions. R denotes regurgitation. Tickmarks along the abcissa represent spurious data points (see text for further discussion) corresponding to rapid bends drawing the polyp outside the focal plane. Large-amplitude variations in length that are not accompanied by a tickmark represent contraction pulses and are not spurious.

frequency shifted from the pre-export level (range of means among replicate polyps: for length, 8.3–9.1 mHz; for volume, 7.9–9.1 mHz) to a lower post-export level (range of means: length, 7.1–7.5 mHz; volume, 6.6–7.5 mHz) in all replicate polyps.

Polyps isolated from a colony

The raw time series for both polyp length and volume (Fig. 6) is conveniently summarized in three intervals:

0–15 minutes post-feeding. As in the case of the coupled

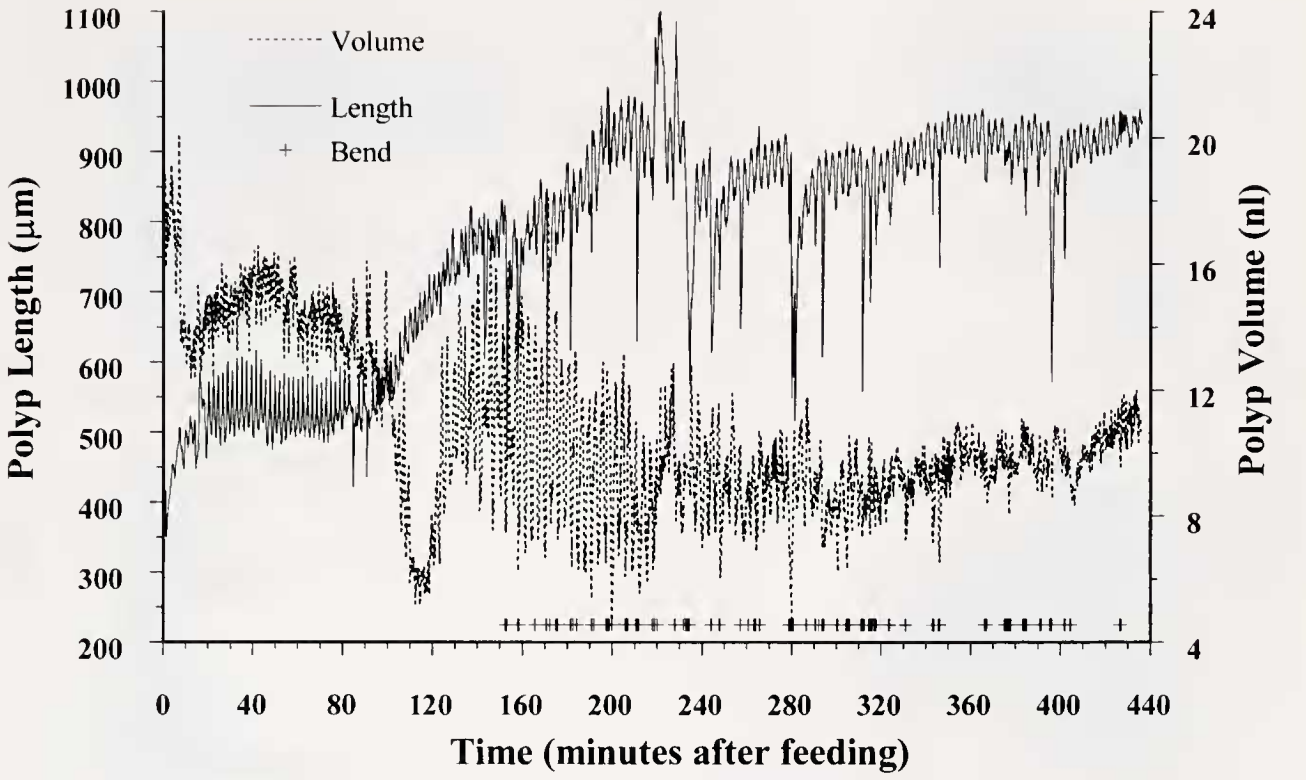

Figure 3. Time series of length (solid line) and volume (dashed line) dynamics of a polyp coupled to a colony by one stolon from 0 to 436.15 min after ingestion of a single brine shrimp nauplius. Tickmarks along the abcissa represent spurious data points (see text for further discussion) corresponding to rapid bends drawing the polyp outside the focal plane. Large-amplitude variations in length that are not accompanied by a tickmark represent contraction pulses and are not spurious.

polyp, feeding resulted in a contraction in polyp length and an increase in volume (not shown). A detailed record of the onset of oscillations immediately after ingestion from a replicate isolated polyp record is shown in Figure 7. As in the coupled treatment (Fig. 3, min 0–20), behavior was irregular for a short time after feeding, and regular oscillations began about 10–15 min post-feeding.

15–763 minutes post-feeding. Like the coupled treatment, the isolated polyp increased in length and volume after feeding (Fig. 6A). As in the coupled case, volume reached a plateau about 40 min. after feeding, whereas the plateau in length was not attained until roughly 150 min post-feeding. The variation in polyp shape 90 min after feeding mirrors that characterizing the early post-feeding period in the coupled treatment, with the greatest variation in polyp width occurring in the hypostome (Fig. 4C). In the isolated case, however, shape also varied substantially at the base of the polyp. Figure 8 compares widths at the polyp base during the period of polyp lengthening (Fig. 8A) with that occurring after the plateau in length has been reached at 150 minutes post-feeding (Fig. 8B). The latter record reveals that the polyp base alternated every other length cycle in maximal and minimal width, which made every other length cycle of greater amplitude (Fig. 8B).

Next, for about 9 h the polyp displayed a trend of gradually increasing length and gradually decreasing volume (Fig. 6A). Regular oscillations in length and volume continued for the entire period. This record is in marked contrast to the coupled treatment, where similar behavior terminated abruptly at about 110 min post-feeding with a large decrease in volume and the onset of large-amplitude volume oscillations. Neither rapid declines in volume nor large-amplitude volume oscillations comparable to those in the coupled case were observed in the isolated case.

763–1474 minutes post-feeding. 763 minutes after feeding, the polyp underwent a 7-min interval of rapid, repeated length contractions, accompanied by variation in volume dynamics (Fig. 6B). From 770 to 790 minutes post-feeding, both length and volume regained values comparable to those that preceded the event at 763 min. The digestive cavity of the polyp had previously been largely opaque; after the event, regions of the cavity became increasingly transparent. This change coincided with a marked alteration in the shape of the polyp as it oscillated. In Figure 9 these

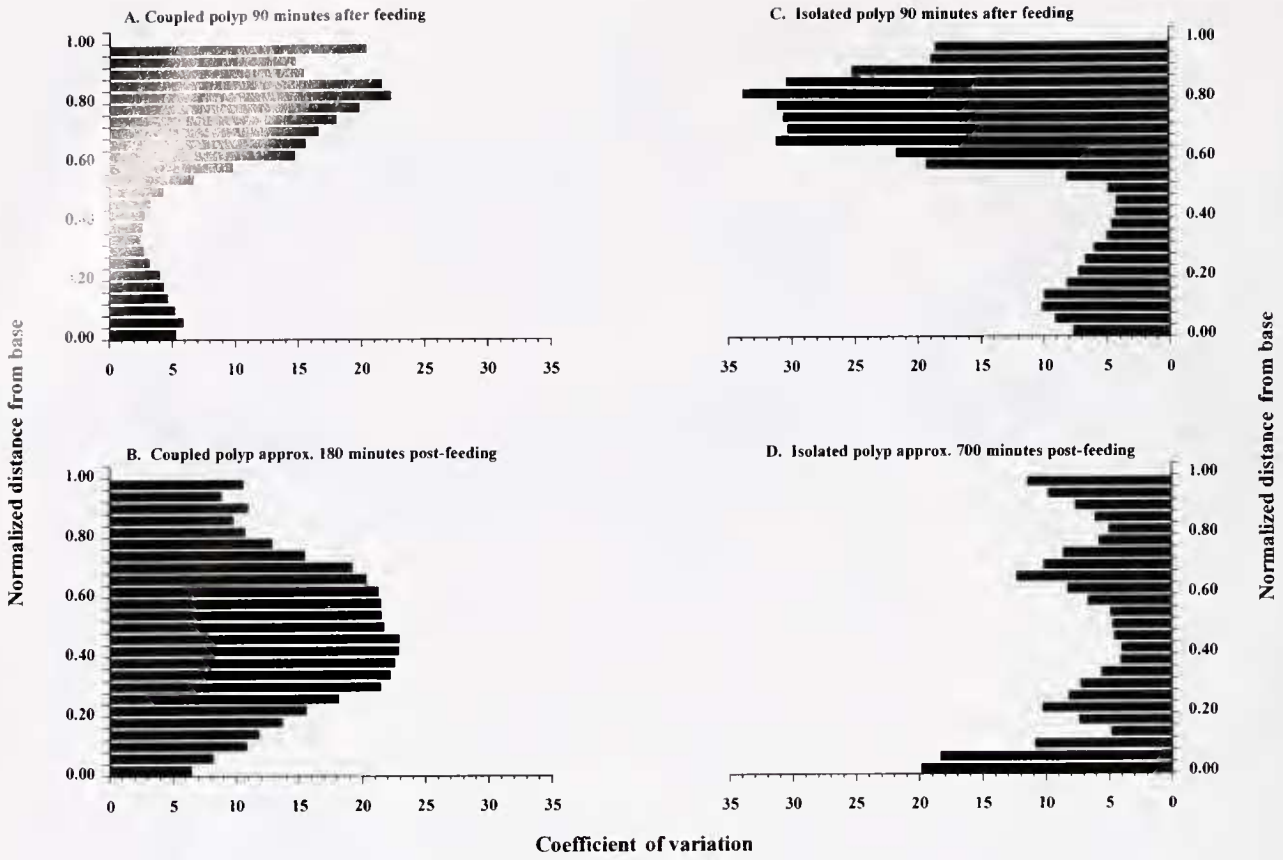

Figure 4. Coefficients of variation from samples of width measures taken every 8 s over a 15-min timecourse at each of 25 loci along the longitudinal axis of a polyp (polyp-stolon junction at 0.00, mouth of polyp at 1.00) for (A) a coupled polyp 90 min after feeding, (B) a coupled polyp 180 min after feeding, (C) an isolated polyp 90 min after feeding, and (D) an isolated polyp 700 min after feeding.

polyp shapes are superimposed on the corresponding record of length and basal width. With every other length maxima the polyp alternated between maintaining a bolus of fluid in the center of the digestive cavity and maintaining two such boli—one in the subtentacular region and one in the basal body column—separated by a constriction in the polyp's center. The same pattern of oscillation is evident in Figure 4D. Variation was maximal in the basal and subtentacular regions of the body column during this interval.

The polyp continued to display regular oscillations in length and volume for an additional 10 h after the event at 763 min (Fig. 6B). Just as in the coupled polyp, contraction pulses and polyp bending became increasingly common in later stages of the record. At 1338–1343 min the polyp regurgitated undigested materials through the mouth and regained a length and volume comparable to those observed prior to feeding (Fig. 6B). Regurgitation in the isolated treatment differed from that in the coupled case (Fig. 2B). In the isolated case, the return to initial conditions was far more abrupt.

The isolated polyp showed a dominant, and remarkably stable, 8-mHz oscillation frequency and a weaker harmonic at 16 mHz that persisted throughout the feeding cycle (Fig. 10). A subharmonic of ~ 4 mHz (*i.e.*, corresponding to events that occurred every other cycle) emerged nearly 150 min after feeding, at the point when basal widths began alternating every other cycle. This subharmonic coexisted with the dominant frequency for the duration of the record. In the period following the event at 763 min (while the polyp displayed movement of fluids between the subtentacular and basal regions of the body column with every other cycle; Fig. 9), the 4-mHz frequency became dominant for 200 min. No appreciable contributions to either length and volume spectra came from frequencies greater than 24 mHz.

The principal features of behavior in isolated polyps were repeatable among replicates (Table I). The principal oscillation frequency varied among replicates (range: 6.7 to 9.0 mHz) but, unlike the frequency in the coupled-polyp treatment, did not shift consistently downward during the post-feeding period. Also, subharmonic frequencies were detected only in the isolated polyps. Finally, the amplitude of

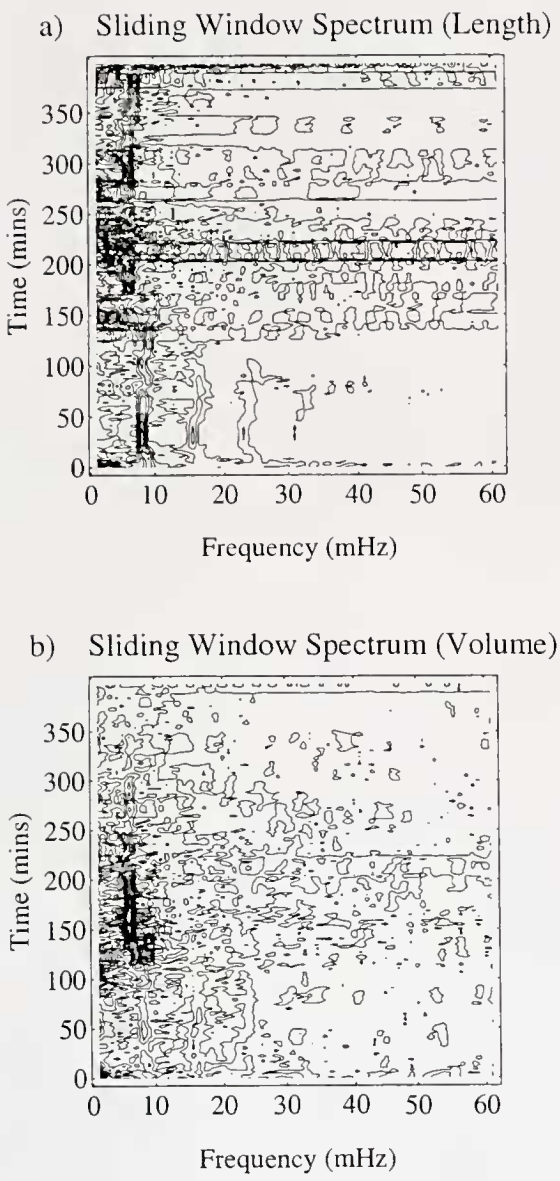

Figure 5. Contour plot, based on the time-series data in Figure 3, of sliding window spectral analysis of (a) length and (b) volume of the coupled polyp. Abcissa represents frequency of oscillation, ordinate represents the sliding window of time (in minutes), and contour lines represent the height of peaks (coming out of the page) that signify the relative importance of a given frequency underlying the cyclic behavior.

volume oscillations was consistently much lower than the larger amplitude volume oscillations characteristic of post-export coupled treatments. (Fig. 3; Table I).

Stolon observations

Feeding was associated with a closing of the polyp-stolonal junction and a momentary cessation of gastrovascular flow in colonies that had been experiencing fluid movement prior to feeding. As the polyp lengthened after the initial contraction, the polyp-stolon junction reopened. The stolon lumen began to oscillate in diameter at 13 and 8 min (on average) in the coupled and isolated treatments respectively: export into the stolon accompanied polyp contraction and import into the polyp accompanied polyp lengthening. The interval between feeding and the onset of stolonal oscillations did not significantly differ from the interval between feeding and the onset of regular oscillations in polyp length and volume (Student's t test; $t = 0.27$, df = 8, $P = 0.80$).

Stolon observations made after this initial period are most conveniently treated separately for the two experimental treatments.

Polyp connected to colony. The frequency of stolon contractions in the first hour after feeding did not differ significantly from the frequency of polyp oscillations (Table II, $t = 0.23$, df = 5, $P = 0.83$). Neither was a significant difference detected in the average lumen diameter of stolons before feeding and in the first hour after feeding (Table II; Student's t test; lumen diameter, $t = 1.19$, df = 4, $P = 0.30$). However, after feeding, stolons contracted significantly more frequently and with greater amplitude than they did before feeding (amplitude, $t = 3.13$, df = 4, $P = 0.03$; frequency, $t = 17.43$, df = 4, $P < 0.01$). Despite the observed export of fluid from the polyp into the stolon, export of particulate matter was only rarely observed in the stolon at this time; on the few occasions when particles were evident, they were few and did not exceed 2 μm in diameter.

The period of interruption in polyp oscillations and decrease in volume, seen at 100 min in the coupled-polyp record, was correlated with events observed on average at 79 min in replicate stolon records. In each stolon replicate, the stolon became greatly expanded with fluid imported from the colony, and the contents of the fed polyp were observed leaving the polyp in a dense stream of large particles (up to 100 μm in length and 15 μm in diameter). Stolonal oscillations changed markedly in the period after export: they were smaller in amplitude and lower in frequency than before export, and the average lumen diameter of the stolens was larger (Table II; lumen diameter $t = 2.88$, df = 4, $P = 0.04$; amplitude, $t = 11.46$, df = 4, $P < 0.01$; frequency, $t = 6.11$, df = 4, $P < 0.01$). Notably, the frequency of stolon oscillations following export mirrored the shift in the frequency of polyp oscillations. Before export, both polyps and stolons oscillated at a frequency of ~8 mHz, whereas after export both oscillated at a frequency of ~6 mHz—the same frequency as in stolons prior to feeding.

Polyp isolated from colony. As in the coupled case, stolon oscillations did not significantly differ in frequency from those observed in polyps ($t = 0.44$, df = 5, $P = 0.68$). Similarly, stolon oscillations prior to export were more frequent and of greater amplitude than stolon oscillations

Table I

Repeatability of length and volume dynamics for coupled and isolated polyps based on observing three replicate polyps in each treatment; values represent means ± standard errors (in parentheses)

	Polyp Length					Polyp Volume				
Pre- or Post-Export	Amplitude (mm)	Principal Frequency (mHz)	Signal : Noise ratio	Subharmonic (mHz)	Signal : Noise ratio	Amplitude (nl)	Principal Frequency (mHz)	Signal : Noise ratio	Subharmonic (mHz)	Signal : Noise ratio
Coupled polyps										
Pre	84.42 (3.71)	8.57 (0.27)	3.69 (1.13)	—	—	4.36 (1.98)	8.30 (0.41)	2.80 (0.69)	—	—
Post	92.43 (18.33)	7.27 (0.13)	2.66 (0.70)	—	—	6.19 (1.59)	7.06 (0.25)	3.31 (0.55)	—	—
Isolated polyps										
Pre	93.56 (3.95)	7.89 (0.67)	5.36 (1.04)	4.14*	2.60*	1.54 (0.08)	7.84 (0.51)	2.08 (0.12)	3.95† (0.16)	2.28 (0.12)
Post	65.11 (8.43)	7.50 (0.42)	2.11 (0.31)	5.14 (0.77)	2.30 (0.13)	1.84 (0.24)	7.93 (0.64)	2.40 (0.86)	3.32 (0.01)	2.08 (0.33)

Pre- and post-export phases of coupled polyps were distinguished visually on the basis of shape variation of the polyp body column while it was oscillating (see Fig. 4a,b); those of isolated polyps were inferred from the coexistence of strong subharmonic frequencies in length or volume and time of occurrence (see text and Fig. 9). Signal-to-noise ratio represents a ratio of a peak height of a frequency to the maximum height of noise in the spectrum.

* Values lacking standard errors indicate that only one replicate displayed a subharmonic.

† Value was based on two replicates instead of three.

prior to feeding, but no difference in average lumen diameter was detected (Table II; lumen diameter $t = 0.42$, df = 4, $P = 0.69$; amplitude, $t = 3.26$, df = 4, $P = 0.03$; frequency, $t = 5.10$, df = 4, $P < 0.01$). Unlike the coupled treatment, however, these oscillations displayed similar average lumen diameters and similar amplitudes and frequencies for 10+ hours post-feeding (Table II). Continuous observation of stolons showed that the isolated polyp, despite the continued fluid exchange with the stolon, exported little particulate matter into the stolon over this extended interval. Three replicate isolated stolon films showed export of a dense stream of large particulates at an average time of 807 min (13.5 h) after feeding, an interval comparable to the event observed in the high-resolution isolated polyp record at 763 min (12.7 h). The average lumen diameter of the stolon after export was not significantly different from that before export, but the oscillations were of smaller amplitude (*i.e.*, stolons remained expanded and filled with particulates throughout oscillation cycles; lumen diameter $t = 1.14$, df = 4, $P = 0.32$; amplitude, $t = 8.40$, df = 4, $P < 0.01$). After export, the frequency of oscillation of the stolon was comparable to that prior to feeding, as well as to that of the stolon in the coupled polyp case after export; but it was distinct from the isolated polyp signal pre- and post-export (Table II).

Discussion

Although it has long been known from anecdotal accounts that hydrozoan polyps undergo periodic changes in shape after ingesting a food item, the results presented above represent, to our knowledge, the first quantitative treatment of this behavior. These data reveal three distinct phases of post-feeding behavior. Phase 1 corresponds to the onset of oscillatory behavior immediately following ingestion, phase 2 to the subsequent period during which the polyp oscillates with limited exchange of particulates with the gastrovascular system, and phase 3 to the interval initiated by the export of particulates from the polyp into the gastrovascular system and terminated by regurgitation. In what follows, we elaborate details of each phase, contrast differences among coupled and isolated polyps, and hypothesize physiological mechanisms for the transitions between behaviors.

Phase 1. In both isolated and coupled treatments, ingestion does not immediately elicit oscillations by the polyp (Figs. 3, 7). Rather, oscillations begin 5–15 min after ingestion and are characterized by a gradual increase in amplitude up to a value which thereafter (phase 2) remains constant. These findings bear on the mechanism that triggers the oscillatory behavior. One obvious candidate for such a trigger is the change in the internal dimensions of the polyp, as might be sensed by stress or strain receptors. Alternatively, the polyp might sense the presence of nutrients or their correlates (*e.g.*, the titer of digestive enzymes). If the former were the case, one would expect polyps to oscillate immediately following ingestion, whereas the latter would imply that oscillation would be delayed by the length of time required for digestion to release nutrients and digestive enzymes. Moreover, if the polyp does respond to some product of digestion, one might expect the titer of such a product to increase gradually as digestion proceeds and, as seen in Figures 3 and 6A for length, the oscillations to increase in amplitude as the titer increases, up to some threshold set by the size of the polyp.

Phase 2. At the end of phase 1, oscillations are constant in amplitude and their frequency does not differ between

isolated and coupled treatments (Table I). During phase 2, polyps of both treatments display comparable patterns of shape variation (Fig. 4A, C) and similar frequencies and relative amplitudes of stolon oscillations (Table II). Although the polyp exchanges fluid with the stolon throughout this interval, particulate exchange is only rarely observed in either treatment. The similarity of the coupled and isolated polyp records during this period suggests that coupled polyps are behaving as autonomous elements.

The treatments, however, differ markedly in the duration of phase 2. Isolated polyps retain this behavior for ~13 h (Fig. 6, Table II), whereas coupled polyps undergo an abrupt transition to phase 3 at 1.5–2 h (Fig. 3, Table II). The difference in duration between the two treatments may reflect a simple mechanical limit: a minimum pressure differential between the polyp and the hydrorhiza may be required to move large particulates through the polyp-stolon junction. If so, the long duration of phase 2 in the isolated polyp may reflect the time required to solubilize food items to the extent that pressure differentials generated by a single polyp are sufficient to drive particulates through the junction. Conversely, the short duration of phase 2 in the coupled case may reflect the far greater pressure differentials associated with colonywide behavior (see below).

Beginning in phase 2, isolated polyps display a trend of gradually decreasing volume (*e.g.*, Fig. 6, *ca.* 0.3 nl/h) that continues until regurgitation. This gradual decrease in volume likely reflects the transfer to endodermal cells that is associated with digestion (Schierwater *et al.*, 1992); the increase in length of the stolon lumen that is associated with tip growth; and perhaps, leakage. Estimating the extent of the latter will require monitoring of endodermal cell volume and stolon length, which we have not attempted here.

Phase 3. Phase 3 is initiated by the export of dense streams of particulate material from the polyp into the stolon. Phase 3 differs between the isolated and coupled cases, as might be expected from the differences between the gastrovascular systems to which the polyps are exporting. In the coupled case, fluid is exchanged with an entire colony. The volume of the colonial gastrovascular system is very large relative to that of the fed polyp, and the colony possesses many other polyps which themselves oscillate to drive large fluid volumes to effect exchanges with the fed polyp. In contrast, the isolated polyp is exporting to a gastrovascular system that lacks other polyps and whose total volume is but a fraction of its own. These differences are interpreted to underlie both the differences and the commonalities in phase 3 between the isolated and coupled treatments.

In the coupled case, phase 3 is marked by an abrupt decline in polyp volume (Fig. 3). In the stolon records this decline is correlated with a large import of fluid from the colony and subsequent export of the contents of the fed polyp into the colonial gastrovascular system (Table II). Export is followed by the onset of regular high-amplitude oscillations in volume that have a frequency distinct from that displayed in phase 2 (Fig. 5) and identical to that of the stolon oscillations in phase 3 (Table II). The repeated appearance of these features in all coupled records (Table I), their absence in all isolated records (Table I), and the temporal correlation of these events with distinctive signatures in stolon records (Table II) lead us to interpret phase 3 in the coupled case as a colonywide exchange distinct from the autonomous behavior displayed during phase 2. Phase 3 is also accompanied by changes in the way that polyp shape varies when oscillating (Fig. 4), and this transition is likewise attributable to the large-volume fluxes associated with exchange of particulates with the colony. Prior to export, the prey fills the gastric cavity; hence, most of the variation in volume is attributable to changes in the dimensions of the hypostome. The gastric cavity is emptied during export to the stolon; thereafter, its shape is presumably limited only by its own extensibility. Finally, with multiple polyps contributing to volume exchange with the fed polyp, the frequency of oscillation may be expected to be determined not by the polyp's autonomous rhythm, but by a frequency characteristic of fluxes through the stolon (Table II).

In the isolated case, phase 3 is similarly marked by the export of particulate matter from the polyp into the stolon, but without the large volume fluxes observed in the coupled case. Since the volume of the gastrovascular system in the isolated case is only a fraction of that of the polyp, the absence of large-volume fluxes and associated variations in polyp shape to accommodate such fluxes is expected. Another notable difference between isolated and coupled cases is that the oscillation frequency of isolated polyps does not change during phase 3 to the frequency characteristic of the stolon (Fig. 10), as it does in the coupled case (Fig. 5). Phase 3 in the isolated case retains the same two frequencies, ~4 and ~8 mHz, that were established at the end of phase 1 and retained throughout phase 2, although the predominant frequency shifts to the subharmonic in phase 3 (Fig. 10, Table I). These differences are likewise interpreted as a consequence of the differences in volume fluxes between the two cases. In the coupled case, the principal force driving fluid movement is the activity of the colony communicating with the fed polyp through the stolon. In the isolated case, the fed polyp remains the principal driving force in exchange with the stolon. The shift between the subharmonic and principal frequencies likely derives from similar considerations. Prior to export, the gastric cavity is rich in particulates, which constrains variation in shape; following export this constraint is released and shape variation associated with the 4-mHz phase 3 signal predominates (Figs. 4D, 9; Table I). Finally, the fact that the stolon in the isolated case oscillates at a frequency different from that of the isolated polyp and identical to that of the post-

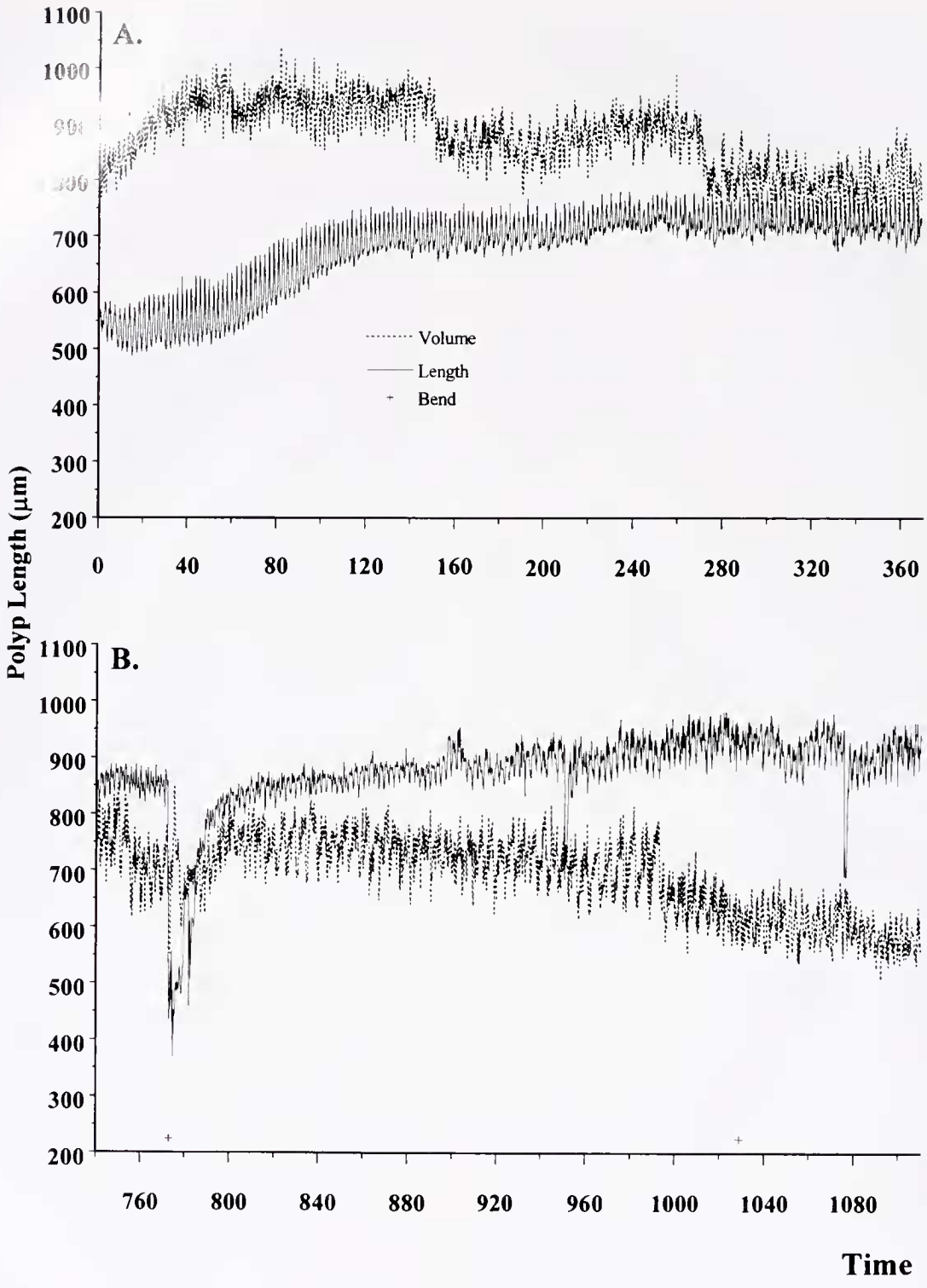

Figure 6. Time series of length (solid line) and volume (dashed line) dynamics of an isolated polyp after ingestion of a single brine shrimp nauplius from (A) 0 to 740 min and (B) 740 to 1474.2 min. R denotes regurgitation. Tickmarks along the abcissa represent spurious data points (see text for further discussion) corresponding to rapid bends drawing the polyp outside the focal plane. Large-amplitude variations in length that are not accompanied by a tickmark represent contraction pulses and are not spurious.

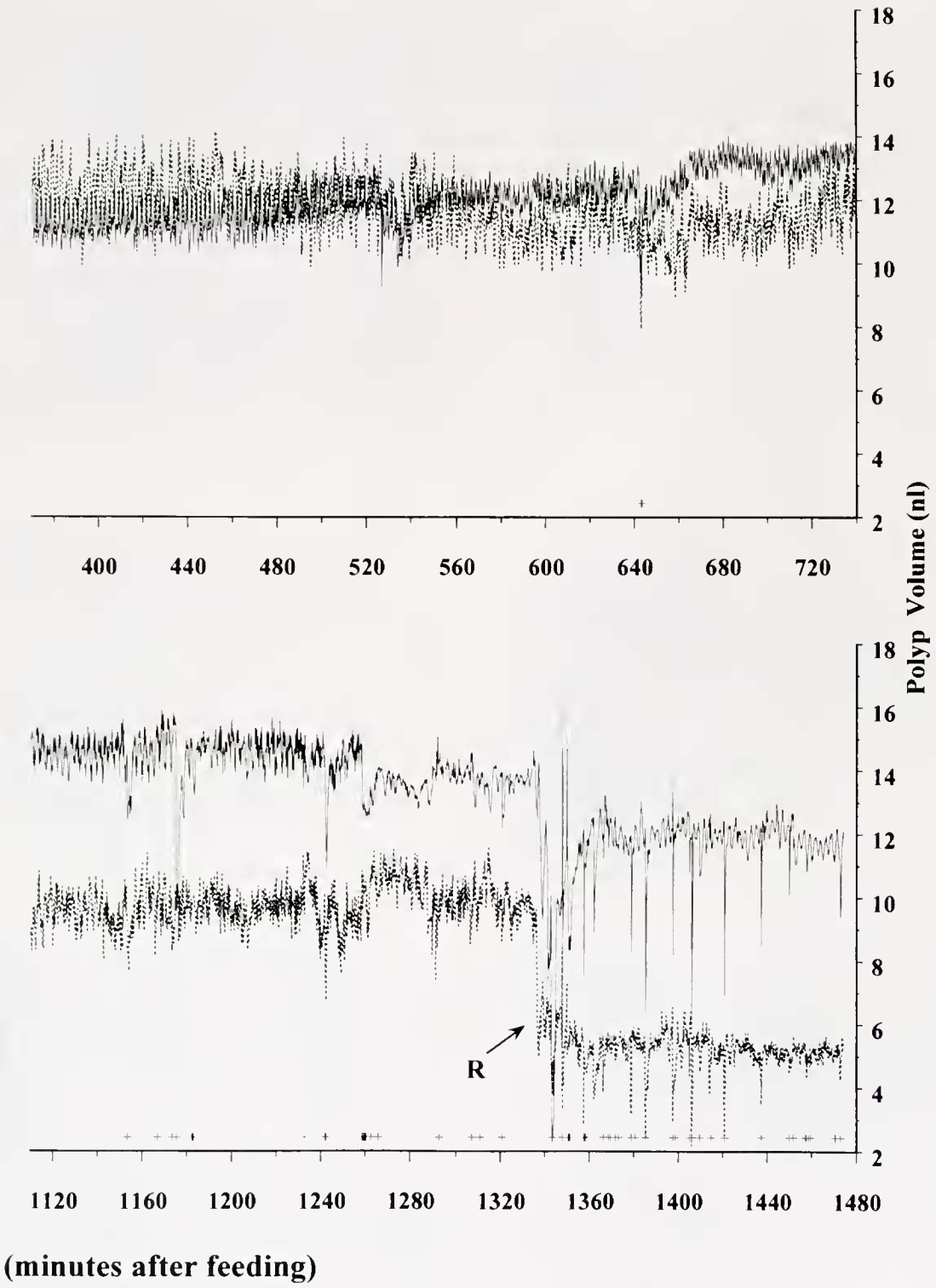

Figure 6. (*Continued*)

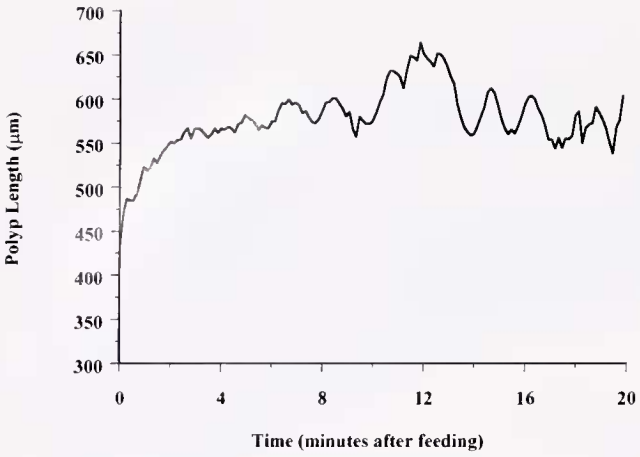

Figure 7. Time series, in minutes after ingestion, of polyp length showing the commencement of regular oscillations of an isolated polyp.

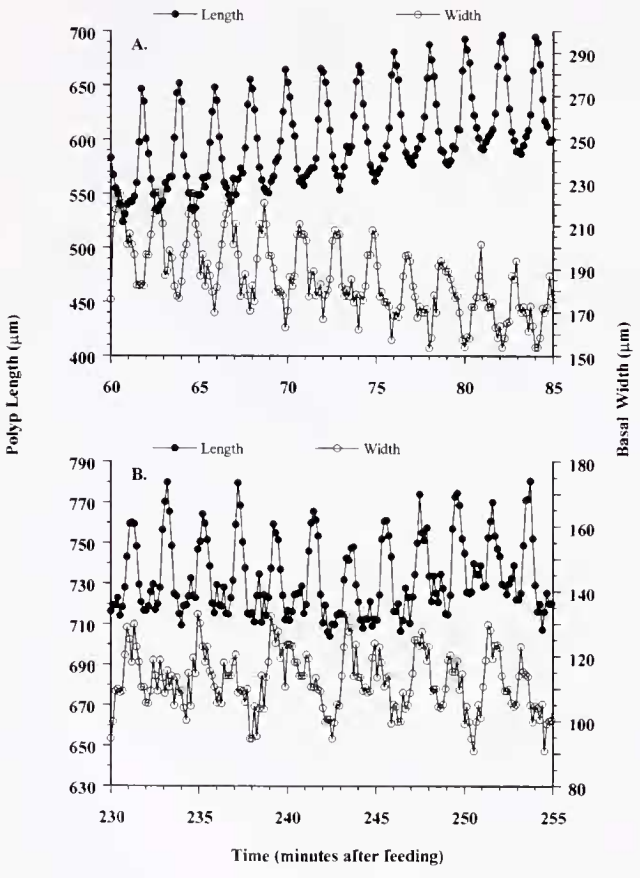

Figure 8. Development of the subharmonic associated with basal width alternating every other length cycle in the isolated polyp record. (A) Polyp length (filled circles) and width (open circles) at the basal-most section for 12 cycles from a representative period (60 to 86 min) when the polyp is lengthening from 0 to 150 min post-feeding. (B) Polyp length (filled circles) and width (open circles) at the basal-most section for 12 cycles from a representative period (230 to 255 min) > 150 min following the development of the 4-mHz subharmonic.

export coupled case strongly suggests the existence of hydrorhizal-specific dynamics (Table II). Indeed, previous observations have established that isolated stolons (*i.e.*, stolons without polyps) in *Hydractinia symbiolongicarpus* exhibit endogenous oscillatory dynamics (Buss and Vaišnys, 1993).

In both treatments, the contraction pulses and rapid polyp bends become increasingly frequent during phase 3 (Figs. 3, 6), consistent with known suppression of contraction pulses during digestion (Passano and McCullough, 1962, 1964; Josephson and Mackie, 1965; Shibley, 1969; Stokes, 1974). The interaction between the contraction pulse system and the digestive oscillations we characterize here bears further attention. Winfree (1970) has shown that a key feature of certain nonlinear oscillators is the capacity for the oscillation to be terminated by perturbations occurring at specific

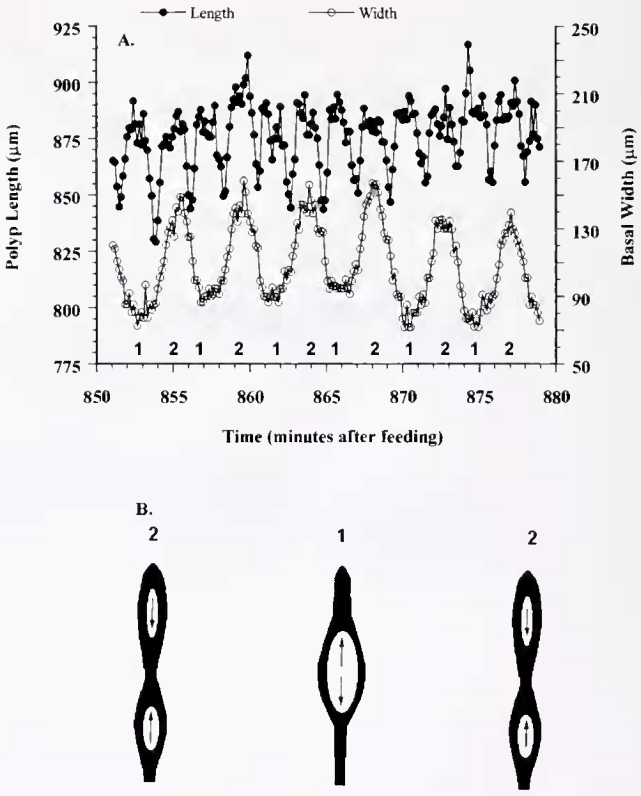

Figure 9. Polyp oscillations during the dominant period by the 4-mHz subharmonic following the 763-min event in the isolated polyp. (A) The length (filled circles) and basal-most width (open circles) of the isolated polyp for 12 cycles from 851 to 878 min after feeding that is representative of the period when the subharmonic dominates the power spectrum. (B) Schematic illustrations of the pattern of shape change of the bolus of transparent fluid in the digestive cavity during three consecutive length maxima of the polyp. Numbers above the polyp correspond to those along the abcissa in (A) that indicate the appearance of the polyp at the maximal polyp length of each cycle. Schematics redrawn from frame-grabbed images during this interval. Arrows within boli inside polyp gastric cavity in (B) indicate the direction of movement of the bolus during the subsequent oscillation cycle.

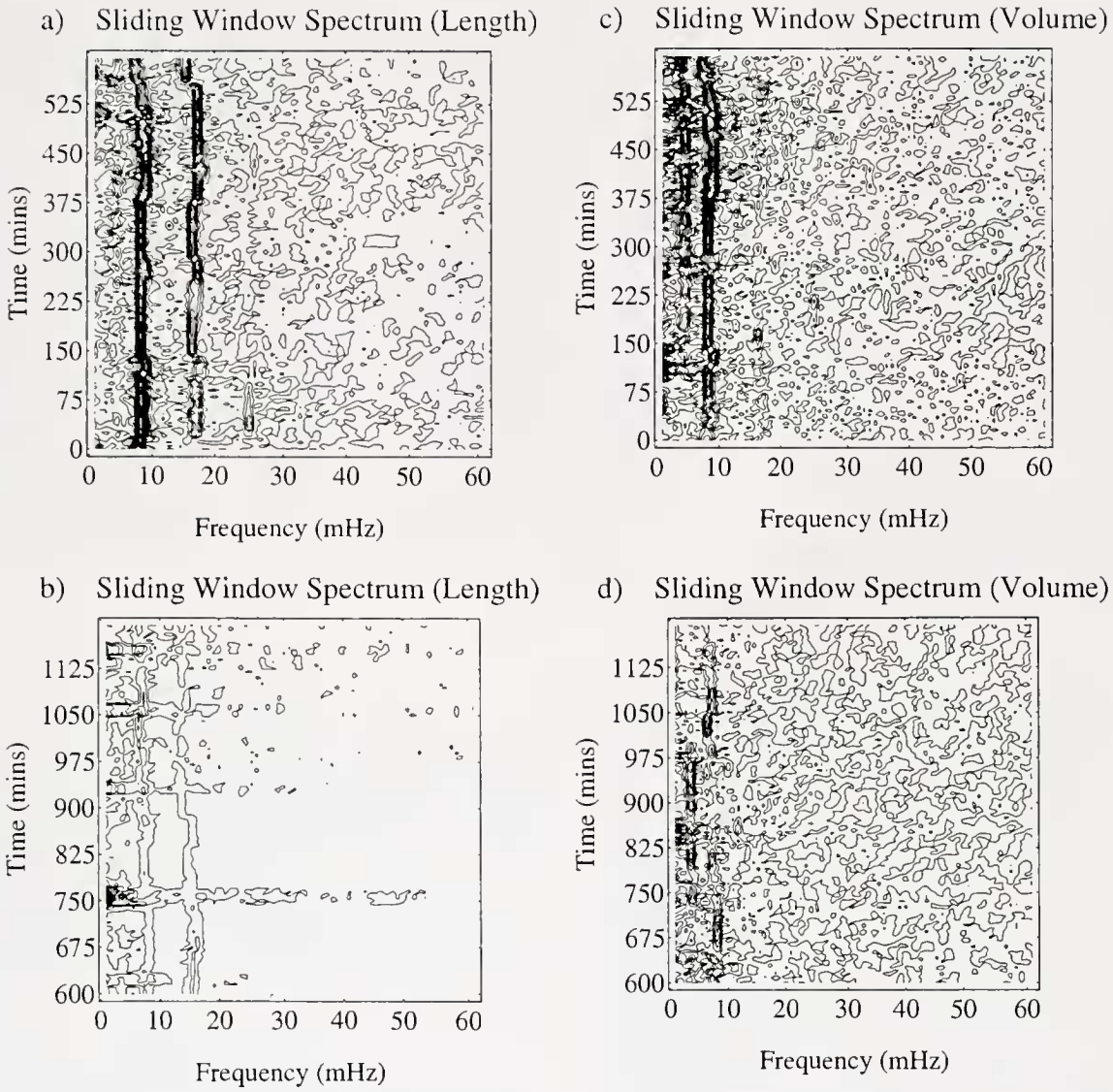

Figure 10. Contour plot, based on the time-series data presented in Figure 6, of sliding window spectral analysis of the isolated polyp for length from (a) 1 to 600 min, and (b) 601 to 1200 min, and for volume from (c) 1 to 600 min, and (d) 601 to 1200 min after ingestion. Abcissa represents frequency of oscillation, ordinate represents the sliding window of time (in minutes), and contour lines represent the height of peaks (coming out of the page) that signify the relative importance of a given frequency underlying the cyclic behavior.

phase relationships. Taddei-Ferretti and Cordella (1976) have shown that contraction pulses can be experimentally annihilated in the predicted fashion. It is conceivable that feeding annihilates contraction pulses and, similarly, that the contraction pulses which reappear in phase 3 annihilate digestive oscillations by this mechanism.

Phase 3 is terminated at comparable times in both the isolated and coupled treatments by regurgitation through the mouth, followed by a return of length and volume to values characteristic of pre-feeding conditions. The dynamics of regurgitation differ between isolated and coupled polyps (*cf.* Figs. 2B and 6B). Whereas regurgitation in the coupled case is not a conspicuous feature of either the length or volume record, regurgitation in isolated polyps is abrupt. The isolated polyp exhibits several rapid, large contractions in length and an associated decline to half of its previous volume. Coupled polyps regurgitate less material that appears more finely particulate, whereas the contractions of isolated polyps are associated with the export of larger pieces of undigested debris. We attribute the differences between treatments in the behavior of polyps and the nature of the material regurgitated to the vastly larger colonial gastrovascular system with its many additional polyps from which undigested particles could be regurgitated.

Table II

Characteristics of oscillations of stolons in the isolated and coupled polyp treatments; values represent the mean and standard errors (in parentheses) of three replicates in each treatment

	Isolated Polyp			Coupled Polyp		
Onset of Oscillations (min)		8.34 (4.99)			13.19 (11.87)	
Export to Hydrorhiza (min)		807.33 (203.95)			78.67 (12.50)	
Stolon Oscillations	Lumen Diameter	Amplitude	Frequency (mHz)	Lumen Diameter	Amplitude	Frequency (mHz)
Pre-feeding	0.29 (0.03)	0.07 (0.03)	5.69 (0.29)	0.24 (0.02)	0.11 (0.03)	5.63 (0.13)
Pre-export						
(30 min post-ingestion)	0.32 (0.06)	0.23 (0.04)	8.48 (0.46)	0.20 (0.03)	0.19 (0.02)	8.40 (0.10)
(150 min post-ingestion)	0.37 (0.05)	0.25 (0.02)	8.64 (0.43)			
Post-export	(Time of export + 60 minutes)			(150 minutes post-ingestion)		
	0.45 (0.05)	0.05 (0.01)	6.00 (0.21)	0.32 (0.03)	0.07 (0.01)	6.07 (0.37)

Data for onset of oscillations and export to hydrorhiza are presented in minutes after ingestion. Means and standard errors for lumen diameter, amplitude, and frequency estimated from the sample of means of each replicate determined from measures taken over three consecutive cycles. Lumen diameter and amplitude are dimensionless indices calculated using the following formulas:

Lumen diameter = (max + min lumen diameter)/(2 × periderm diameter)

Amplitude = max − min lumen diameter/periderm diameter

A theoretical model. These findings suggest a simple conceptualization of the feeding response of an isolated hydrozoan polyp. The principal phases of behavior reflect differing input-output relationships between the polyp and either the external (*via* the mouth) or internal (*via* the polyp-stolon junction) environment. Inputs in the form of food items elicit oscillatory behavior (phase 1), which leads to the output of fluid, but few particulates, to the stolonal system (phase 2). The final phase begins with the export into the stolon of particulates (phase 3) and is terminated by export of undigested material (regurgitation) from the mouth and subsequent return to initial conditions. These data lead us to suggest that an input of food releases elicitors (*e.g.*, nutrients or digestive enzymes) whose action triggers an underlying biochemical system (*e.g.*, ion potentials at neuromuscular junctions), and that the oscillation of that system is reflected in corresponding oscillations in length and width. An ordinary differential equation model of a nonlinear oscillator that can undergo a supercritical Hopf bifurcation as the concentration of an elicitor is increased has been shown to be capable of reproducing principal features of the isolated polyp data presented here (Wagner *et al.*, 1998). Elaboration of such a single-polyp model is easily imagined based on the hypothesis that elicitors are circulated in gastrovascular fluids during phase 2 and that when these elicitors reach a threshold value they trigger oscillations of adjacent polyps, thereby generating the behavior described above for a coupled polyp. These considerations suggest that a spatially distributed system of coupled nonlinear oscillators is a reasonable abstraction of the gastrovascular system of a hydrozoan colony.

Acknowledgments

We thank Dr. Arvydas Matiukas for his development of early versions of the algorithms for this project, Dr. Harald Freund for advice in developing the volume analysis algorithm, and Jim Bonacum for technical assistance. We thank Neil Blackstone and an anonymous reviewer for improving the quality of this manuscript. This research was supported by the National Research Council Twinning Program and the National Science Foundation (OCE-93-15082) to Leo Buss.

Literature Cited

Berrill, N. J. 1953. Growth and form in gymnoblastic hydroids. VI. Polymorphism within the Hydractiniidae. *J. Morphology* **92:** 241–272.

Bevan, J. A., G. Kaley, and G. M. Rubanyi (eds.) 1995. *Flow-Dependent Regulation of Vascular Function.* Oxford Univ. Press, Oxford, UK.

Blackstone, N. W. 1997. A dose-response relationship for experimental heterochrony in a colonial hydroid. *Biol. Bull.* **193:** 47–61.

Blackstone, N. W. 1998. Physiological and metabolic aspects of experimental heterochrony in colonial hydroids. *J. Evol. Biol.* **11** (in press).

Blackstone, N. W., and L. W. Buss. 1992. Treatment with 2,4-dinitrophenol mimics ontogenetic and phylogenetic changes in a hydractiniid hydroid. *Proc. Natl. Acad. Sci. USA* **89:** 4057–4061.

Blackstone, N. W., and L. W. Buss. 1993. Experimental heterochrony in hydractiniid hydroids: why mechanisms matter. *J. Evol. Biol.* **6:** 307–327.

Buss, L. W., and J. R. Vaišnys. 1993. Temperature stress induces dynamical chaos in a cnidarian gastrovascular system. *Proc. Roy. Soc. Lond.* **B 252:** 39–41.

Buss, L. W., and P. O. Yund. 1989. A sibling species group of *Hydractinia* in the northeastern United States. *J. Mar. Biol. Assoc. UK* **69:** 857–875.

Dudgeon, S. R., and L. W. Buss. 1996. Growing with the flow: on the

maintenance and malleability of colony form in the hydroid *Hydractinia*. *Am. Nat.* **147:** 667–691.

Josephson, R. K., and G. O. Mackie. 1965. Multiple pacemakers and the behavior of the hydroid *Tubularia*. *J. Exp. Biol.* **43:** 293–332.

LaBarbera, M. 1990. Principles of design of fluid transport systems in Zoology. *Science* **249:** 992–1000.

Murray, C. D. 1926. The physiological principle of minimum work applied to the angle of branching of arteries. *Proc. Natl. Acad. Sci. USA* **12:** 835–841.

Passano, L. M., and C. B. McCullough. 1962. The light response and the rhythmic potential of *Hydra*. *Proc. Natl. Acad. Sci. USA* **48:** 1376–1382.

Passano, L. M., and C. B. McCullough, 1964. Coordinating systems and behavior in *Hydra*. II. The rhythm potential system. *J. Exp. Biol.* **42:** 205–231.

Press, W. H., S. A. Teukolsky, W. T. Vetterling, and B. P. Flannery. 1992. *Numerical Recipes in C*. Cambridge University Press, New York.

Priestley, M. B. 1981. *Spectral Analysis and Time Series*. Academic Press, New York.

Schierwater, B., B. Piekos, and L. W. Buss. 1992. Hydroid stolonal contractions mediated by contractile vacuoles. *J. Exp. Biol.* **162:** 1–21.

Sherman, T. F. 1981. On connecting large vessels to small. *J. Gen. Physiol.* **78:** 431–453.

Shibley, G. A. 1969. Gastrodermal contractions correlated with rhythmic potentials and pre-locomotor burst in *Hydra*. *Am. Zool.* **9:** 586.

Stokes, D. R. 1974. Physiological studies of conducting systems in the colonial hydroid *Hydractinia echinata* 1. Polyp specialization. *J. Exp. Zool.* **190:** 1–18.

Taddei-Ferretti, C., and L. Cordella. 1976. Modulation of the *Hydra attenuata* rhythmic activity: phase response curve. *J. Exp. Biol.* **65:** 737–751.

Wagner, A., S. R. Dudgeon, J. R. Vaišnys, and L. W. Buss. 1998. Non-linear oscillations in polyps of the colonial hydroid *Podocoryne carnea*. *Naturwissenschaften* **85:** 117–120.

Winfree, A. T. 1970. An integrated view of the resetting of a circadian clock. *J. Theor. Biol.* **28:** 327–374.

Zamir, M. 1977. Shear forces and blood vessel radii in the cardiovascular system. *J. Gen. Physiol.* **69:** 449–461.